Rapid-Release Griffithsin Fibers for Dual Prevention of HSV-2 and HIV-1 Infections

Kevin M. Tyo,[a,b] Amanda B. Lasnik,[b] Longyun Zhang,[b,c] Alfred B. Jenson,[d] Joshua L. Fuqua,[a,b] Kenneth E. Palmer,[a,b,d,e] Jill M. Steinbach-Rankins[a,b,c,d,e]

[a]Department of Pharmacology and Toxicology, School of Medicine, University of Louisville, Louisville, Kentucky, USA
[b]Center for Predictive Medicine, Louisville, Kentucky, USA
[c]Department of Bioengineering, Speed School of Engineering, University of Louisville, Louisville, Kentucky, USA
[d]James Graham Brown Cancer Center, University of Louisville School of Medicine, University of Louisville, Louisville, Kentucky, USA
[e]Department of Microbiology and Immunology, School of Medicine, University of Louisville, Louisville, Kentucky, USA

Kenneth E. Palmer and Jill M. Steinbach-Rankins are co-senior authors.

ABSTRACT The biologic griffithsin (GRFT) has recently emerged as a candidate to safely prevent sexually transmitted infections (STIs), including human immunodeficiency virus type 1 (HIV-1) and herpes simplex virus 2 (HSV-2). However, to date, there are few delivery platforms that are available to effectively deliver biologics to the female reproductive tract (FRT). The goal of this work was to evaluate rapid-release polyethylene oxide (PEO), polyvinyl alcohol (PVA), and polyvinylpyrrolidone (PVP) fibers that incorporate GRFT in in vitro (HIV-1 and HSV-2) and in vivo (HSV-2) infection models. GRFT loading was determined via enzyme-linked immunosorbent assay (ELISA), and the bioactivity of GRFT fibers was assessed using in vitro HIV-1 pseudovirus and HSV-2 plaque assays. Afterwards, the efficacy of GRFT fibers was assessed in a murine model of lethal HSV-2 infection. Finally, murine reproductive tracts and vaginal lavage samples were evaluated for histology and cytokine expression, 24 and 72 h after fiber administration, to determine safety. All rapid-release formulations achieved high levels of GRFT incorporation and were completely efficacious against in vitro HIV-1 and HSV-2 infections. Importantly, all rapid-release GRFT fibers provided potent protection in a murine model of HSV-2 infection. Moreover, histology and cytokine levels, evaluated from collected murine reproductive tissues and vaginal lavage samples treated with blank fibers, showed no increased cytokine production or histological aberrations, demonstrating the preliminary safety of rapid-release GRFT fibers in vaginal tissue.

KEYWORDS griffithsin, HIV-1, HSV-2, drug delivery, fibers, microbicide

The worldwide incidence of human immunodeficiency virus type 1 (HIV-1) and herpes simplex virus 2 (HSV-2) remains a persistent challenge to global health. It is estimated that over 36 million and 500 million people worldwide are impacted by HIV-1 and HSV-2, respectively, with an estimated 5,500 new cases of HIV-1 infections each day (1, 2). Moreover, studies have shown that HSV-2 increases the risk of HIV-1 acquisition as much as 2- to 4-fold (3, 4). Despite ongoing efforts to reduce sexually transmitted infections (STIs), women remain disproportionately affected by HIV and HSV-2, and to date neither infection is curable (5).

In response to these challenges, recent efforts have focused on both oral and topical preexposure prophylaxis (PrEP) with antiretroviral drugs (ARVs) to reduce the risk of HIV-1 infection. However, the success of oral PrEP is dependent upon regimented administration and corresponding user adherence, with adverse effects often resulting from sustained use and the high doses of ARVs needed to achieve efficacy with oral

Address correspondence to Jill M. Steinbach-Rankins, jill.steinbach@louisville.edu.

PrEP (5, 6). In contrast, topical PrEP employs localized administration to the female reproductive tract (FRT) and often necessitates lower administered doses. Yet current topical PrEP delivery platforms, such as gels and films, have similarly struggled with low user adherence in several clinical trials (7). In the FEM-PrEP and MTN-003 clinical trials, which required patients to adhere to daily administration regimens, adherence was evident in less than 40% and 57% of the study participants, respectively (8, 9), prompting the consideration of new dosage forms. In addition, the use of traditional ARVs has elicited concerns regarding drug resistance and toxicity (10, 11); moreover, few ARVs are efficacious against both HSV-2 and HIV-1 infections, requiring the codelivery of multiple active agents to provide dual-purpose protection. These limitations have led to the development of new active agents and delivery platforms to provide effective and dual-purpose prevention.

Given the challenges with ARVs, there has been a growing interest in the use of biologics to prevent viral infections, particularly candidates that exhibit dual-purpose protection against HSV-2 and HIV-1. Proteins such cyanovirin-N and scytovirin and polysaccharides such as carrageenan have demonstrated moderate success in viral inhibition by binding to viral glycoproteins (12). However, some of these biologics have been shown to elicit inflammatory responses, which may limit the utility of these agents for STI prevention (13). In recent work, the lectin griffithsin (GRFT) (14–19) has emerged as one the most potent biological microbicide candidates, demonstrating efficacy in the picomolar range against HIV-1. This potent efficacy is due to the ability of GRFT to bind to multiple carbohydrates on the surface of viral glycoproteins gp120, gp41, and gp160, thereby inhibiting virus entry and cell-to-cell transmission of HIV-1 (20). Furthermore, GRFT has been shown to disrupt the cell-to-cell spread of HSV-2 and has demonstrated efficacy in murine models of HSV-2 infection (21). Due to its outstanding safety and efficacy in both human cells and murine models (22), GRFT is currently being evaluated in clinical trials.

Similar to other active agents which have demonstrated efficacy against STIs, GRFT formulations are currently being developed in the form of gels, tablets, and films. However, these platforms may suffer from poor user adherence, seen specifically in gels due to product leakage, which may contribute to reluctance to use prior to intercourse. In fact, previously developed ARV (tenofovir) and biologic (carrageenan) gel combinations have shown disappointing results in clinical trials specifically due to poor user adherence (23, 24), suggesting the need for alternative dosage form options for women. One potential solution is the development of a fiber-based platform, composed of solid yet flexible materials, to minimize leakage, enable discreet administration, improve user adherence, and provide on-demand (administered within 24 h) dual protection against HSV-2 and HIV-1 infections. Additionally, studies have shown that fibers may increase the retention of incorporated agents within the reproductive tract (25), potentially improving user preference and efficacy.

Within the past decade, fiber-based platforms have emerged as promising intravaginal delivery alternatives. In one of the first studies to develop fibers for intravaginal application, cellulose acetate phthalate fibers demonstrated pH-responsive release of tenofovir disoproxil fumarate (TDF) to inhibit HIV-1 infection (26). In other studies, polymeric fibers and fiber blends provided high encapsulation of ARVs, including maraviroc, raltegravir, and tenofovir, and sustained release for up to 30 days (27–32). In addition, our group demonstrated short-term and sustained release of the antiviral agents TDF and acyclovir to prevent HIV-1 and HSV-2 infections (33, 34). However, few studies have focused on delivery vehicles that can deliver potent multipurpose biologics like GRFT (21, 35, 36). Consequently, we have more recently focused on the development of new biological options, including pH-responsive (37) and surface-modified (38) fibers that incorporate GRFT, to inhibit both HSV-2 and HIV infections.

In this study, our goals were to develop rapid-release electrospun fibers that incorporate the biologic GRFT to provide on-demand dual-purpose protection against HIV-1 and HSV-2 infections *in vitro* and to demonstrate initial safety and efficacy against HSV-2 infection *in vivo*. Rapid-release fibers, composed of polyethylene oxide (PEO),
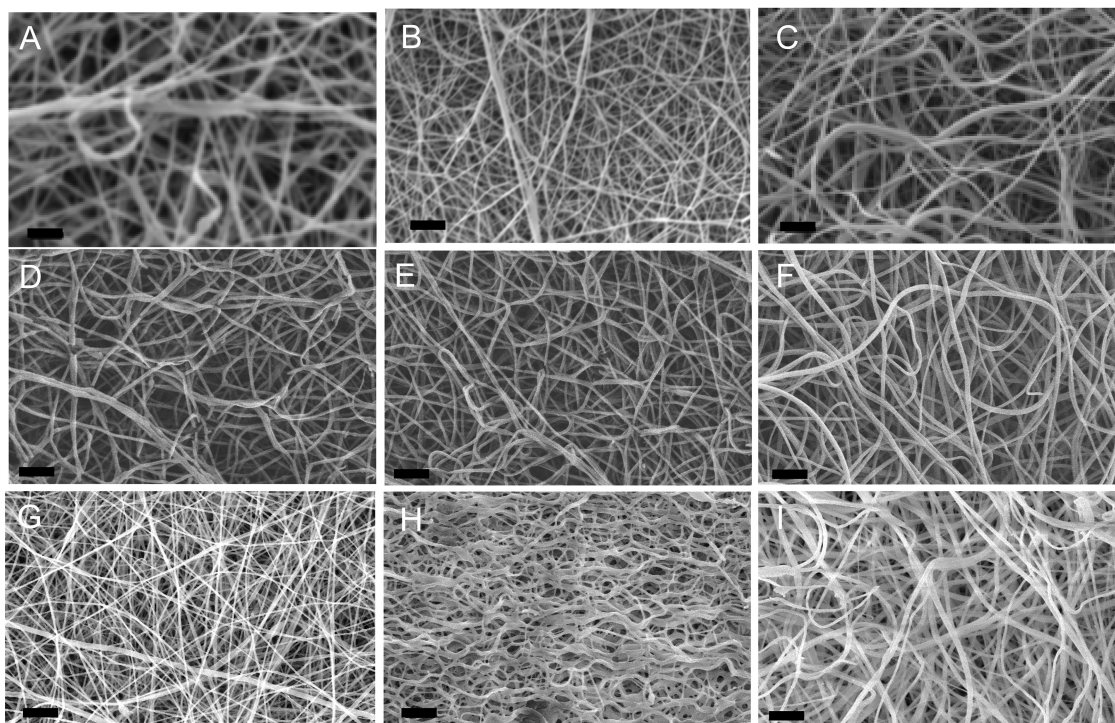
FIG 1 Scanning electron microscopy (SEM) images of blank (A to C), 1% (wt/wt) GRFT (D to F), and 10% (wt/wt) GRFT (G to I) fibers. (A) 5% PEO blank fibers; (B) 20% PVA blank fibers; (C) 20% PVP blank fibers; (D) 5% PEO fibers incorporating 1% (wt/wt) GRFT; (E) 20% PVA fibers incorporating 1% (wt/wt) GRFT; (F) 20% PVP fibers incorporating 1% (wt/wt) GRFT; (G) 5% PEO fibers incorporating 10% (wt/wt) GRFT; (H) 20% PVA fibers incorporating 10% (wt/wt) GRFT; (I) 20% PVP fibers incorporating 10% (wt/wt) GRFT. Scale bars represent 2 μm.

polyvinyl alcohol (PVA), and polyvinylpyrrolidone (PVP), were selected due to their established biocompatibility, mucoadhesivity, and rapid dissolution in aqueous environments (39–42). The ability of GRFT fibers to provide complete protection against both HIV-1 and HSV-2 infections was demonstrated *in vitro*. Furthermore, the efficacy of GRFT fibers was assessed in a murine model of lethal HSV-2 infection, and it was demonstrated that a single application of PEO, PVA, or PVP GRFT fibers provided potent protection when administered 4 h prior to infection. In addition, histology and cytokine expression data, assessed from murine reproductive tissues and vaginal lavage samples, demonstrated the preliminary safety of rapid-release GRFT fibers in vaginal tissue.

RESULTS

Fiber size and morphology. The morphology of blank and GRFT PEO, PVA, and PVP fibers is shown in Fig. 1. All fibers demonstrated well-rounded fiber morphology, with average diameters ranging from 220 to 507 nm (see Table S1 in the supplemental material). The addition of 1% (wt/wt) GRFT to PEO and PVP fibers resulted in significantly decreased diameters of 239 and 242 nm, while no statistical significance was observed between blank PVA and 1% GRFT PVA fibers that shared similar diameters regardless of GRFT incorporation. The addition of 10% (wt/wt) GRFT produced fibers with diameters spanning 243 to 339 nm, demonstrating a statistically significant increase in fiber diameter for 10% (wt/wt) GRFT PVA and PVP fibers relative to 1% (wt/wt) GRFT PVA and PVP fibers. However, PEO fiber diameters remained unchanged with additional GRFT incorporation. Within similarly loaded GRFT fibers, statistical significance in fiber diameter was observed between the 10% GRFT PEO and PVA fibers, while no statistical significance was observed across the 1% (wt/wt) GRFT formulations.

Fiber characterization. GRFT loading was assessed using an ELISA (Fig. 2). For 1% (wt/wt) GRFT PEO, PVA, and PVP fibers, GRFT loading ranged from 7.4 to 9.7 μg GRFT/mg fiber, exhibiting no statistical significance between formulations. For 10%
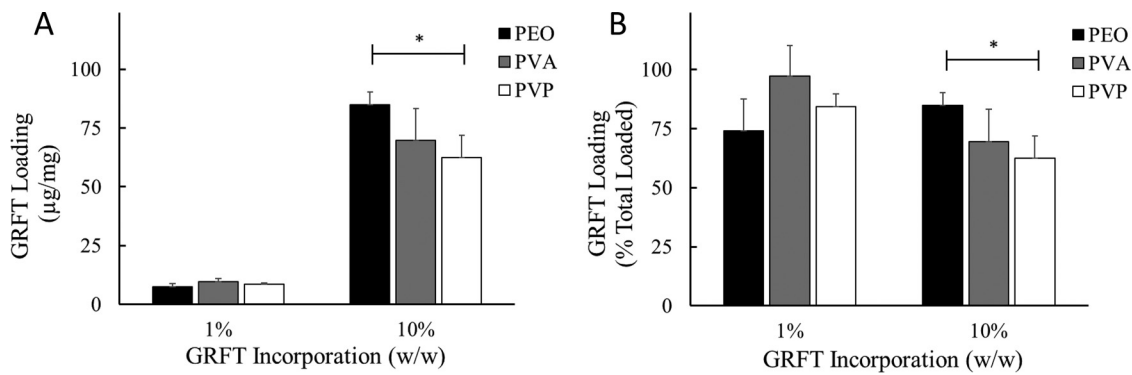
FIG 2 GRFT loading in different hydrophilic fiber formulations. Eluates from GRFT fibers dissolved in PBS were used to determine GRFT loading via ELISA. GRFT loading is expressed as the mean ± standard deviation of triplicate readings of three independent fiber batches. Statistical significance between fiber formulations with the same loading is shown (*, $P < 0.05$).

(wt/wt) GRFT PEO, PVA, and PVP fibers, GRFT loadings were 84.8, 69.6, and 62.4 μg GRFT/mg fiber, respectively, with PEO fibers demonstrating statistically higher loading than PVP fibers. Correspondingly, the encapsulation efficiencies for each fiber formulation ranged from 74.0 to 97.2% and from 62.4 to 84.2% for 1 and 10% GRFT fibers, respectively, demonstrating consistently high GRFT loading and suggesting electrospinning compatibility between the polymer and lectin. There were no observable trends between GRFT encapsulation efficiency and fiber diameters.

In vitro **HIV-1 and HSV-2 inhibition from GRFT fibers.** The dual-purpose antiviral activity of 1% (wt/wt) GRFT fibers was determined using HIV-1 pseudovirus and HSV-2 plaque inhibition assays. For HIV-1 inhibition studies, all fibers demonstrated complete and dose-dependent HIV-1 inhibition (Fig. 3A and B). The half-maximal inhibitory
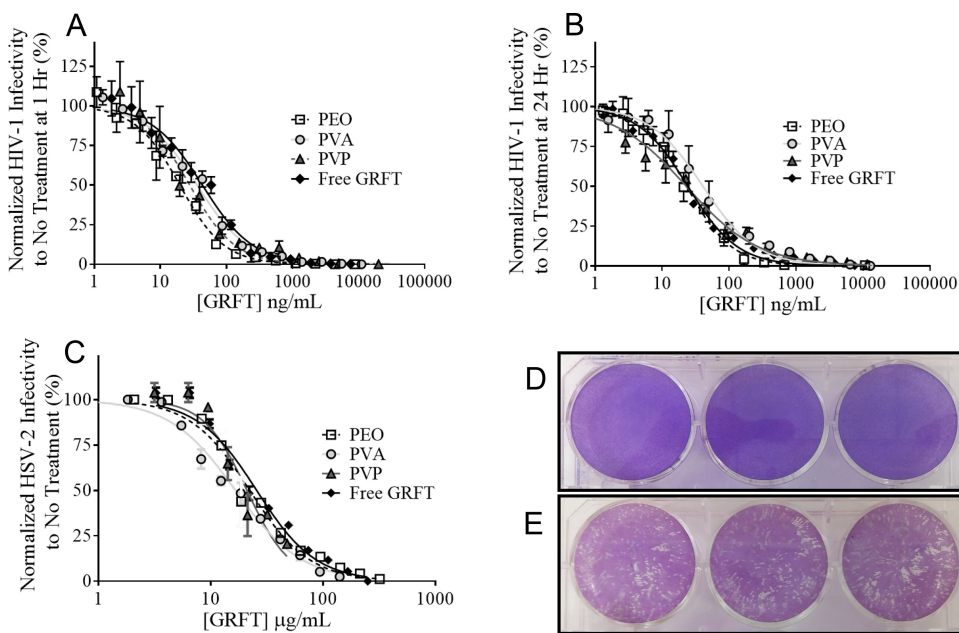

FIG 3 GRFT fibers demonstrate complete protection against *in vitro* HIV-1 and HSV-2 infections. Three independent batches of 1% (wt/wt) GRFT fibers were assessed for the ability to inhibit HIV-1 infection. Fiber eluates were incubated with cells 1 h (A) and 24 h (B) prior to HIV-1 infection. GRFT released from all three fiber formulations achieved complete efficacy against HIV-1 infection, similarly to free GRFT. (C) *In vitro* HSV-2 plaque assays were performed using 10% (wt/wt) GRFT fibers, which achieved complete efficacy against HSV-2 infection *in vitro*, similarly to free GRFT. (D and E) Wells treated with GRFT fibers showed decreased plaque sizes and numbers (D) relative to those of untreated (or blank fiber-treated [data not shown]) cells infected with HSV-2 (E). The percent infection relative to untreated/infected control groups for both HIV-1 and HSV-2 assays is shown as the mean ± standard deviation of triplicate readings.

TABLE 1 IC$_{50}$ values from *in vitro* HIV-1 and HSV-2 infectivity assays[a]

Fiber formulation	1-h HIV-1 IC$_{50}$ (ng/ml)	24-h HIV-1 IC$_{50}$ (ng/ml)	1-h HSV-2 IC$_{50}$ (μg/ml)
PEO	17.9 ± 5.4	17.3 ± 7.2	22.0 ± 2.1
PVA	26.7 ± 7.7	21.7 ± 14.8	16.6 ± 0.9*
PVP	26.6 ± 2.7	23.5 ± 14.1	21.0 ± 2.4
Free GRFT	24.1 ± 15.6	22.8 ± 12.2	25.5 ± 0.5

[a]GRFT eluates from rapid-release fibers were assessed against HIV-1 and HSV-2 infections and compared to free GRFT. Fibers demonstrated activity comparable to that of free GRFT. No statistical significance between groups was observed in HIV-1 inhibition studies as a function of fiber formulation or with respect to administration time. In HSV-2 plaque inhibition assays, GRFT PVA fibers demonstrated lower IC$_{50}$ values than other formulations and free GRFT-treated controls ($P < 0.05$). The average IC$_{50}$ values are expressed as the means ± standard deviations. Statistical significance between GRFT PVA fibers and free GRFT is shown (*, $P < 0.05$).

concentration (IC$_{50}$) values for PEO, PVA, and PVP fibers administered 1 and 24 h prior to infection ranged from 17.3 ± 7.2 to 26.7 ± 7.7 ng/ml, compared to 24.1 ± 15.6 and 22.8 ± 12.2 ng/ml for free GRFT at 1 and 24 h, respectively (Table 1). No statistical significance was observed between the IC$_{50}$ values of GRFT PEO, PVA, and PVP fibers, suggesting no differences in efficacy based on polymer type or as a function of administration time with respect to cell infection. Moreover, similar inhibition values relative to free GRFT indicate that the electrospinning process maintains the functional activity of GRFT.

Plaque assays were used to assess the ability of GRFT fibers to inhibit HSV-2 infection. Fibers containing a higher concentration of GRFT (10% [wt/wt]) were evaluated, due to the increased concentration of GRFT needed to inhibit HSV-2, relative to HIV-1, infection. GRFT PEO, PVA, and PVP fibers demonstrated protection against HSV-2 infection equivalent to that of free GRFT (IC$_{50}$, 25.5 ± 0.5 μg/ml), with IC$_{50}$s of 22.0 ± 2.14, 16.6 ± 0.92, and 21.0 ± 2.4 μg/ml (Fig. 3C). No statistical significance in efficacy was observed between GRFT fibers and free GRFT, except for PVA fibers, which showed a lower IC$_{50}$ value than that of free GRFT ($P < 0.05$ [Table 1]). Moreover, administration of all GRFT fiber formulations resulted in decreases in both plaque number and size relative to those of untreated/infected controls (Fig. 3D and E).

***In vitro* cytotoxicity.** To assess the cytotoxicity of rapid-release fibers, 3-(4,5-dimethyl-2-thiazolyl)-2,5-diphenyl-2H-tetrazolium bromide (MTT) assays were conducted using VK2/E6E7 (VK2), Ect1/E6E7, End1/E6E7, TZM-bl, and Vero E6 cell lines. All cell lines incubated with 1 and 10% (wt/wt) GRFT fibers demonstrated greater than 93% viability after 24, 48, and 72 h of fiber administration, relative to untreated cells (Fig. 4). No statistical significance in cell viability as a function of polymer type or GRFT loading was observed.

***In vivo* efficacy against HSV-2 infection.** The antiviral efficacy of rapid-release GRFT fibers was assessed in a murine model of lethal HSV-2 infection. A single dose of 10% (wt/wt) GRFT fibers was intravaginally administered to female BALB/c mice, followed by a single HSV-2 challenge with 5,000 PFU (90% lethal dose [LD$_{90}$]), 4 h after fiber insertion (Fig. 5A and B). Mice were evaluated daily for progression of HSV-2 infection for 14 days postinfection (Fig. 5C). Mice that were administered GRFT fibers (PEO, PVA, or PVP) exhibited statistically significant decreases in HSV-2 infectivity, with 85, 95, and 100% survivability, respectively, in contrast to untreated infected controls (5% survivability; $P < 0.05$), and exhibited protection comparable to that of free GRFT ($P \geq 0.05$). Additionally, while the administration of blank PEO fibers imparted protection to 50% of mice, they demonstrated a statistically significant decrease in prevention relative to that in GRFT fiber-treated (PEO, PVA, or PVP) or free GRFT-treated mice ($P < 0.05$) and a statistically significant increase in protection relative to that in untreated infected mice ($P < 0.05$). Kaplan-Meier survival curves for each independent experiment are shown in Fig. S1 in the supplemental material.

Another important finding from this study was the difference in infection progression between untreated/infected mice and mice treated with GRFT fibers (Fig. 6). The first symptoms of HSV-2 infection in mice typically manifest 4 to 5 days postinfection,
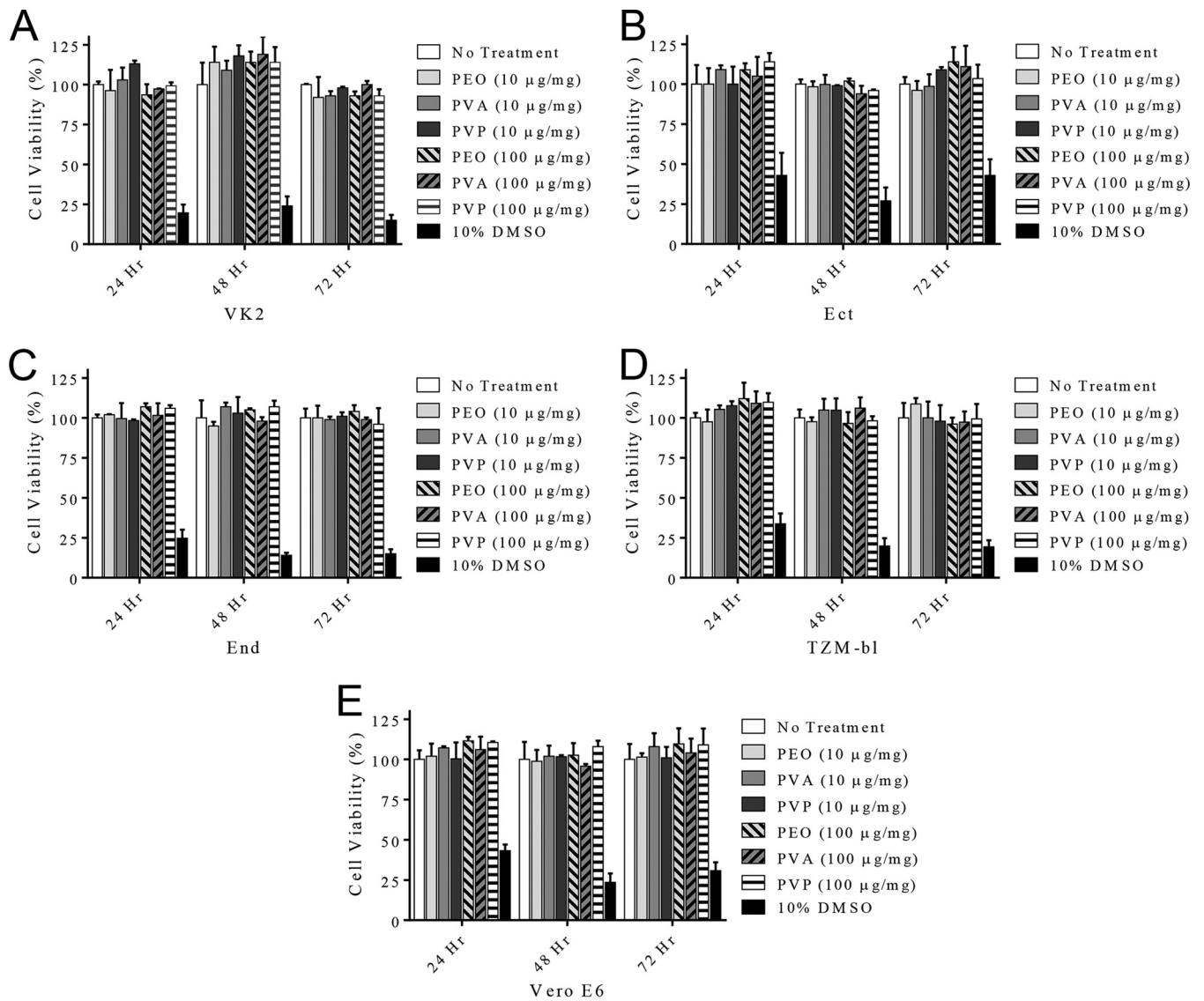
FIG 4 The cytotoxicity of PEO, PVA, and PVP fibers administered to vaginal VK2/E6E7 (A), Ect1/E6E7 (B), End1/E6E7 (C), TZM-bl (D), and Vero E6 (E) cells for 24, 48, and 72 h was assessed using the MTT assay. Greater than 93% viability was observed across all cell lines for all fiber formulations.

during which time mice exhibit symptoms of localized swelling in the vaginal area and decreased hind leg mobility. After 5 to 8 days, ~75% of mice from the untreated infected control group required euthanasia due to the rapid progression and severity of infection. In contrast, all mice administered GRFT fibers (PEO, PVA, or PVP) or free GRFT that exhibited symptoms showed decreased progression of infection relative to that in untreated/infected mice over the same duration. The mice that did not survive infection despite pretreatment with GRFT fibers or free GRFT (representing up to 15% total mice) exhibited a more gradual progression of infection, requiring euthanasia 7 to 10 days instead of 5 to 8 days postinfection. The prolonged duration of viral quiescence suggests that GRFT may provide partial protection against infection for the few mice that exhibited overt signs of infection. In comparison, the administration of blank fibers showed no change in progression of HSV-2 infection in mice relative to that in untreated infected controls. Finally, for the few infected mice treated with free GRFT (1 of 20) or GRFT PVA fibers (2 of 20), initial symptoms disappeared near of the end of the study. The decreased levels of infection in combination with the more gradual progression demonstrate the ability of GRFT fibers to protect against a lethal dose of HSV-2 after a single application.
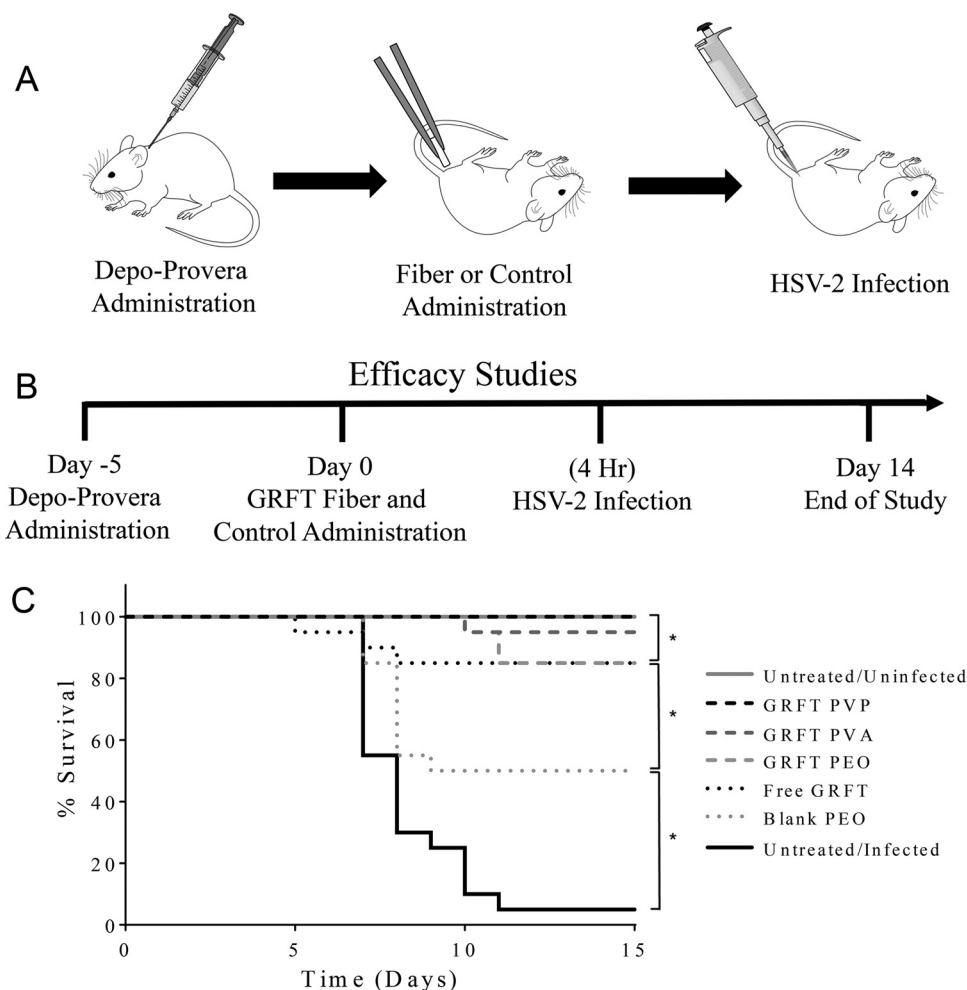
FIG 5 Schematic timetable and Kaplan-Meier survival curves of *in vivo* HSV-2 efficacy study. (A) Sequence of murine treatments over the course of the HSV-2 efficacy study. (B) Timeline of HSV-2 efficacy study. (C) GRFT fibers (10% [wt/wt]) were assessed for the ability to protect mice against a lethal challenge (LD_{90}) of HSV-2 infection ($n = 20$). All GRFT fiber formulations demonstrated strong protection against HSV-2 infection, resulting in 85% to 100% murine survivability. Blank fibers also demonstrated partial protection and showed significant survivability (50%), relative to the untreated infected control group, but imparted significantly less protection than GRFT fibers and free GRFT. In contrast, untreated infected mice demonstrated only 5% survivability. Statistical significance between experimental groups is shown (*, $P < 0.05$).

In vivo safety. To assess the *in vivo* safety of rapid-release platforms, fibers were intravaginally administered to mice, and reproductive tissue and vaginal lavage samples were collected and analyzed 24 and 72 h following administration. Tissue samples were evaluated for possible edema of muscle, interstitial, and epithelial tissue. In addition, untreated and blank fiber-treated cervical and vaginal epithelia morphologies were compared and assessed for possible keratinization and goblet cell presence. Scores ranging from 1 to 4 were used to determine the severity of epithelial changes. Figure 7 shows images of tissues collected 24 h after fiber administration. Extracted tissues from untreated controls demonstrated compact squamous and cervical epithelial tissue, with no evidence of edema or inflammation. Tissues treated with blank PEO, PVA, and PVP fibers showed morphology and normality similar to those of untreated controls (scores of 1 to 2). Furthermore, there was no increase in lymphocyte accumulation in fiber-treated groups. Overall, the tissues from blank fiber-treated mice were comparable to tissues from untreated mice; however, one PVA-treated sample exhibited increased levels of mucin secretion and neutrophil presence (score 3), yet the vaginal and cervical epithelia were intact (Fig. S2A).
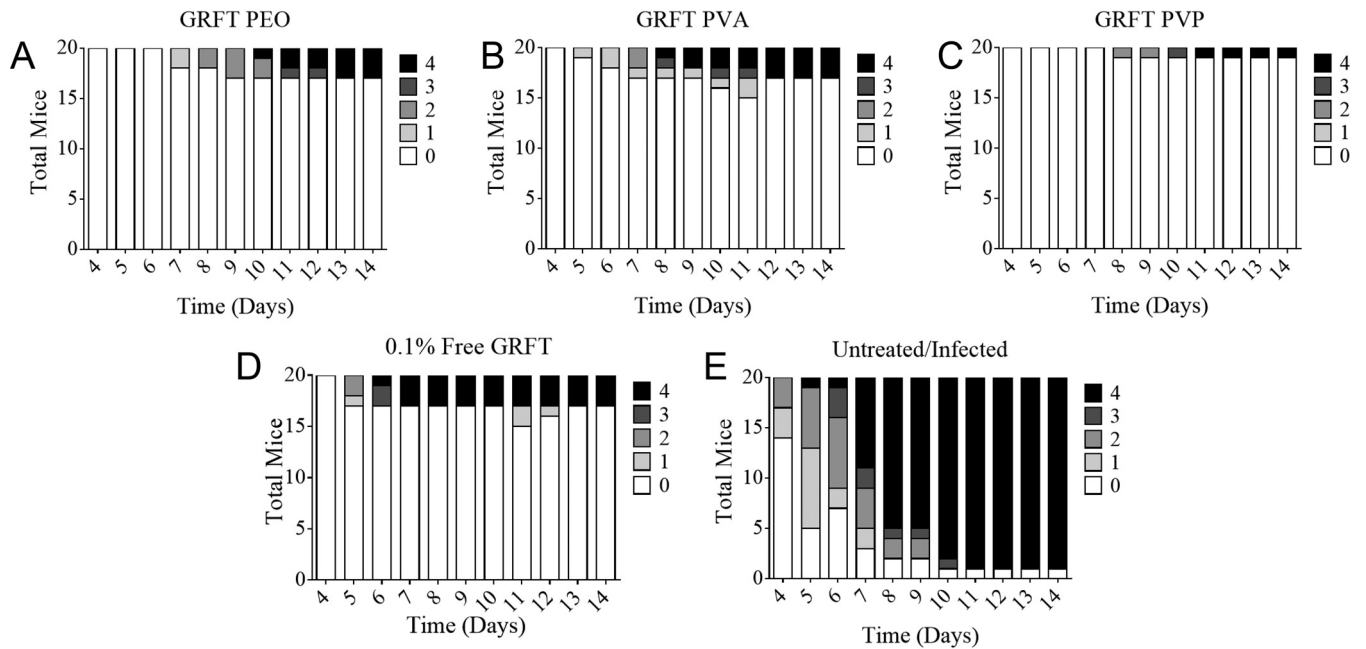
FIG 6 Griffithsin fibers protect mice against HSV-2 infection. Mice were administered 10% (wt/wt) GRFT fibers 4 h prior to HSV-2 infection (LD_{90}). Mice were evaluated and scored for progression of infection once daily for 14 days postinfection. Infected mice were administered PEO (A), PVA (B), and PVP (C) GRFT fibers, as well as free GRFT (D) or no treatment (E). Mice administered GRFT fibers and free GRFT exhibited decreased severity of infection, as well as more gradual progression of infection, relative to that of untreated infected animals.

For nonoxynol-9 (N-9)-treated mice, a slight increase in neutrophil accumulation was observed on the surface of the cervical squamous epithelium relative to that in untreated controls, indicating minor topical damage (score range of 1 to 3). Murine tissue from one N-9-treated mouse exhibited increased inflammation, due to the presence of peripheral blood mononuclear cells, goblet cell fusions, and epithelial disruption, resulting in a score of 3 (Fig. S2B). As for sham-treated mice, there was a slight increase in neutrophil accumulation after 24 h in most samples relative to that in
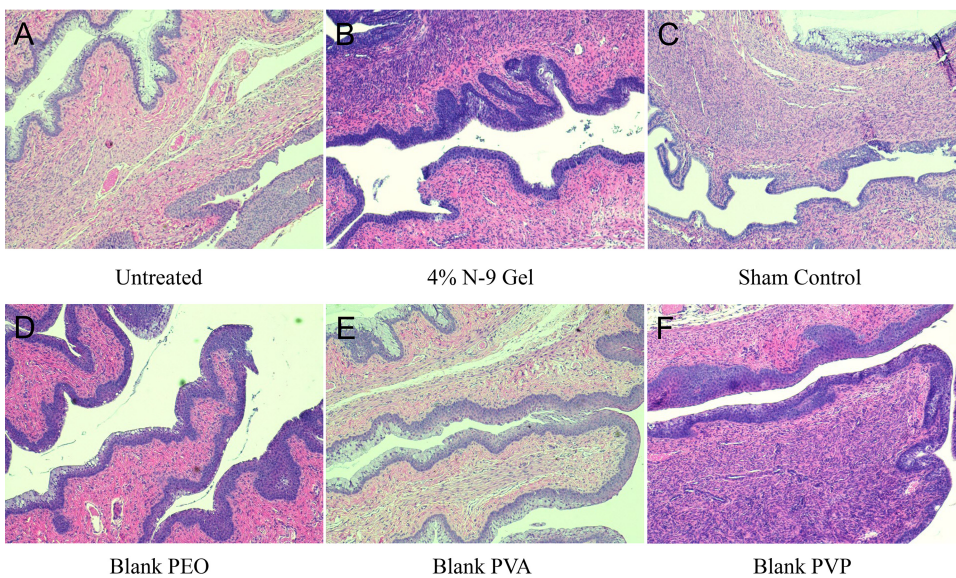
FIG 7 The *in vivo* safety of rapid-release fibers was assessed by intravaginally administering fibers for 24 h. Images depict H&E-stained tissues of murine reproductive tracts exposed to no treatment (A), N-9 gel (B), and sham treatment (C), as well as blank PEO (D), PVA (E), and PVP (F) fibers for 24 h. There was no indication of tissue inflammation or epithelial disruption from fiber administration relative to the case with untreated controls.
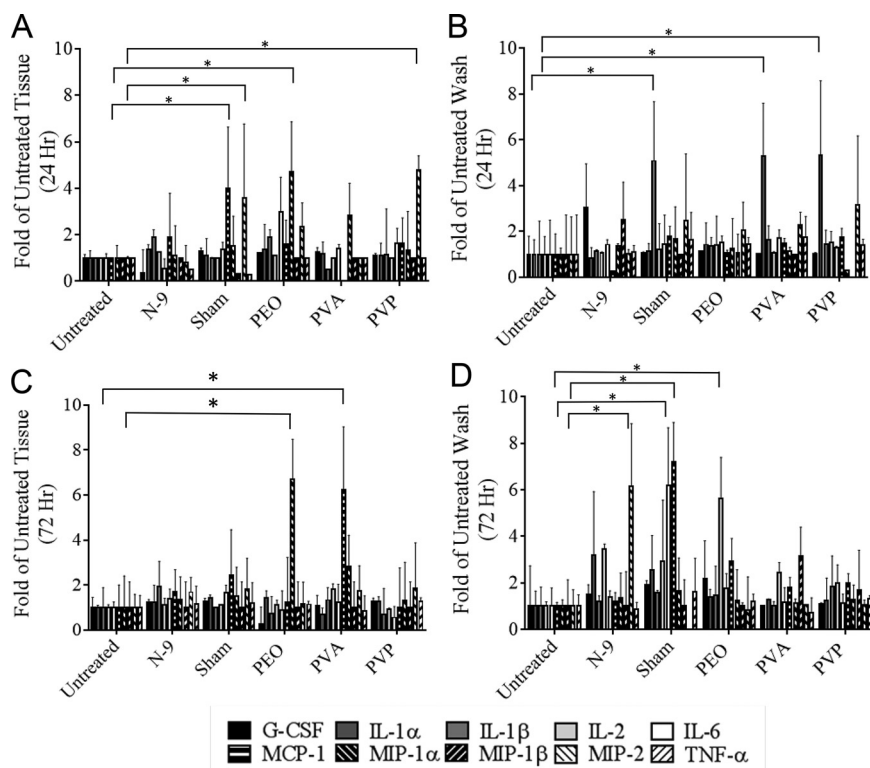
FIG 8 Cytokine expression from extracted murine tissue and vaginal lavage samples collected 24 (A and B) and 72 (C and D) h after fiber administration. Cytokine expression was assessed concurrently with histology to determine the preliminary safety of rapid-release fibers in a murine model. Mice treated with blank fibers expressed cytokine levels similar to those of untreated controls, indicating that the presence of fibers does not induce inflammation or an inflammatory response (*, $P < 0.05$).

untreated controls (score range of 1 to 2), and one sham-treated replicate was noted for widespread neutrophil accumulation, indicating tissue repair (score 3). However, alterations present in both N-9- and sham-treated controls were not observed in 72-h tissue samples (Fig. S3), perhaps indicating transitory damage.

Cytokine expression from murine FRTs and vaginal lavage samples was assessed 24 and 72 h after blank fiber administration. Cytokine expression was compared to those in untreated, N-9-treated, and sham-treated mice based on previously published guidelines, in which a significant level of intravaginal inflammation results in more than a 2- to 5-fold increase in cytokine expression relative to that in untreated controls (22). Figure 8 summarizes the results from the cytokine analysis; they show that blank fibers do not induce proinflammatory or immune-regulatory cytokine expression. In fiber-treated tissue and vaginal lavage samples, cytokine levels were found to be comparable to those in tissue and washes collected from untreated control groups. Cytokine expression levels were similar in both 24- and 72-h samples, with 11 of 13 cytokines within a range of 2- to 5-fold expression of untreated controls. A few exceptions were observed using the above criteria: vaginal lavage samples collected 24 h after PVA and PVP fiber administration demonstrated a 5-fold increase in interleukin 1α (IL-1α) expression, while vaginal tissue collected 24 h after PEO and PVP administration demonstrated elevated levels of MIP-1α and MIP-2, respectively, relative to those in untreated controls ($P < 0.05$). Additionally, vaginal tissue collected 72 h after PEO fiber administration demonstrated a 6-fold increase in monocyte chemoattractant protein (MCP-1) and MIP-1α expression relative to those in untreated controls ($P < 0.05$). For sham-treated controls (sham treatment simulated the administration method via tweezers only), increased cytokine expression was observed in 24-h tissue (MIP-2), 24-h wash (IL-1β), and 72-h wash (IL-6 and MCP-1) relative to that in untreated controls. N-9-treated samples demonstrated an increase in MIP-2 expression in 72-h wash samples

only. Both IP-10 and gamma interferon (IFN-γ) were undetected in vaginal lavage or tissue samples. An enzyme-linked immunosorbent assay (ELISA) used to confirm IL-1β levels showed similar results, in that blank fibers induced negligible increases in cytokine expression relative to that in untreated controls ($P \geq 0.05$).

DISCUSSION

In this study, electrospun fibers composed of hydrophilic polymers were evaluated as an alternative topical delivery platform to provide on-demand dual-purpose protection against HSV-2 and HIV-1 infections. GRFT PEO, PVA, and PVP fibers demonstrated complete *in vitro* efficacy against both HIV-1 and HSV-2 infections and exhibited safety comparable to that of free GRFT and untreated cells when tested in three vaginal cell lines. Furthermore, GRFT fibers were efficacious in an *in vivo* HSV-2 infection model and demonstrated preliminary safety by maintaining macrostructural histology and cytokine expression similar to those in untreated mice. Moreover, fibers preserve the activity of incorporated GRFT and substantiate the feasibility of electrospun fibers to provide an efficacious alternative platform for the intravaginal delivery of griffithsin.

The antiviral lectin GRFT has been shown to potently inhibit a variety of viral infections and has demonstrated particular promise in providing dual-purpose protection against HIV-1 and HSV-2 infections (20, 21). To date, GRFT has been primarily developed as a gel dosage form (21); however, concerns surrounding gel administration, such as leakage and suboptimal user adherence in clinical trials, has prompted research into alternative delivery platforms. Other recent work has begun to evaluate the use of fast-dissolving inserts (FDIs) comprised of the gelling agents carrageenan, hydroxyethyl cellulose, and xanthan gum (35, 36) for the delivery of active agents GRFT and carrageenan. These inserts have shown promise in providing on-demand release of agents, corresponding to immediate inhibition of simian-human immunodeficiency virus (SHIV) infection in macaque models and HSV-2 and human papillomavirus (HPV) inhibition in murine models. Another recent study examined the efficacy of poly(lactide-co-glycolide) GRFT nanoparticles (NPs) (43) that coencapsulate the ARV dapivirine and demonstrated synergistic protection against *in vitro* HIV-1 infections. While these studies show the potential of alternative GRFT delivery platforms, they may also be prone to challenges regarding leakage and ease of administration, prompting the development of solid-dosage-form alternatives that may be easily and discreetly administered to the FRT.

In this work, we envisioned a solid dosage form comprised of PEO, PVA, or PVP polymers, due to their established mucoadhesivity, biocompatibility, and hydrophilicity (44, 45). All three polymers have been used alone or in blends for drug delivery applications, particularly for the delivery of proteins and biologics (46–52). In previous intravaginal delivery studies, mucoadhesive polymers were explored to increase active agent retention (44, 45). Specifically, one study investigated the use of PVA and PVP fibers to increase nanoparticle retention in the murine reproductive tract (25), finding that nanoparticles incorporated within fibers demonstrated a 30-fold increase in retention relative to free NPs (25). In addition, their established biocompatibility suggests their potential for translation, particularly in the reproductive microenvironment. Finally, the hydrophilic properties of PEO, PVA, and PVP enable fiber fabrication using aqueous solutions, which can help to retain GRFT (53) and potentially other biologic activity. We anticipate that the mucoadhesive properties of these polymers will increase GRFT retention within the FRT, thereby enhancing efficacy at potentially lower doses than in other dosage forms such as gels or nanoparticles. Future studies will be conducted to assess how mucoadhesion may enhance GRFT retention within the reproductive tract.

In these studies, the goals were to develop and preliminarily assess the safety and efficacy of rapid-release GRFT fibers in a murine model of HSV-2 infection. PEO, PVA, and PVP fibers all demonstrated high GRFT loading in both the 1 and 10% (wt/wt) GRFT formulations. These results are in agreement with those of other studies that have used hydrophilic fibers to incorporate proteins and other hydrophilic agents (54, 55). The

high encapsulation efficiency of these fibers is attributed in part to the favorable interactions between GRFT and polymers, specifically hydrogen bonding via hydrophilic functional groups (44). This high loading, and moreover the preservation of GRFT activity, was further demonstrated in our *in vitro* efficacy studies, in which GRFT fibers completely inhibited both HIV-1 and HSV-2 infections in a dose-dependent manner, regardless of polymer formulation and with IC_{50} values similar to that of free GRFT.

Previous studies have shown that GRFT exhibits picomolar efficacy against HIV-1, enabling 1% (wt/wt) GRFT fibers to completely prevent HIV-1 infection *in vitro*. However, the decreased number of oligomannose N-linked glycans present on the surface of HSV-2 necessitates a higher dose of GRFT (21) and, correspondingly, GRFT fibers to prevent HSV-2 infection *in vitro*. Despite these differences in GRFT potency against HIV-1 and HSV-2, each fiber formulation provided complete, dual-purpose protection against *in vitro* infections.

Based on these successes, we sought to assess the efficacy and safety after fiber administration in a murine model of HSV-2 infection. In these studies, GRFT fibers were administered 4 h prior to HSV-2 infection. This administration time was based on surveys that studied women's preferences for topical delivery platforms, showing that an "ideal" platform should provide convenient and discreet administration and could be applied hours prior to intercourse (56). In line with previous studies testing GRFT gels (21), all three GRFT fiber formulations provided comparable or enhanced protection in efficacy (LD_{90}) studies (85 to 100% survival) that was comparable to or better than that achieved with free GRFT (85% survival). Moreover, the few mice that became infected showed decreased weight loss and overall slower progression of HSV-2 symptoms relative to those in untreated infected controls, indicating that GRFT fibers may reduce the severity of symptoms and alter the course of infection. This trend of reduced severity and delayed progression was also observed in previous *in vivo* GRFT studies, further validating the efficacy profile of GRFT fibers (18).

Interestingly, blank fiber administration protected up to 50% of total mice, suggesting that physical fiber presence alone (or dissolved polymer) may provide a significant level of barrier-like prevention against infections. Previous studies by our group have demonstrated similar *in vitro* results, suggesting that the fiber itself may act as a barrier to viral infection (34, 38). Future work will seek to better define the fiber characteristics that contribute to this inhibition and utilize this information to improve fiber design. We hypothesize that fibers may be fabricated to serve as physical barriers to limit viral distribution within the FRT, in addition to providing release of incorporated active agents.

Last, we acknowledge that regardless of the protection imparted by GRFT fibers (or free GRFT), a small fraction of mice (averaging 1.3 and 3 mice of 20 for GRFT fiber- and free GRFT-treated mice, respectively) became infected. Previous work has shown similar results, which showed that free GRFT significantly reduces the incidence of infection but may not impart complete protection within a sample group (21). Future work will assess dose dependence and effects of different administration times of GRFT fibers on *in vivo* prevention.

In addition to efficacy, it is critical that fibers are safe to administer and minimize potential inflammatory responses (57, 58). All fiber formulations (PEO, PVA, and PVP) exhibited initial safety in *in vitro* and *in vivo* experiments. Histological analyses suggest the preliminary safety of these platforms *in vivo*, with the majority of fiber-treated tissue showing no signs of cervical or vaginal epithelium disruption or increased neutrophil accumulation relative to that in untreated controls. Additionally, cytokine expression in fiber-treated mice tissues and vaginal lavage samples demonstrated values within the normal range shown in previous studies, suggesting the biocompatibility of both polymers and GRFT (22, 59). Although cytokine values from a few experimental and sham control group tissues were elevated relative to those in untreated controls (as seen with increased levels of IL-1α in PVA and PVP 24-h vaginal lavage samples and increased expression of MCP-1 and MIP-1 in PEO 72-h tissue samples), these incidences may have been due to either vehicle administration or the inherent variability of *in vivo*

studies; however, future studies must be conducted to further determine this. Previous studies have shown that inflammation is characterized by the overexpression of multiple cytokines. For example, increased IL-1α expression is typically associated with increased tumor necrosis factor alpha (TNF-α) or IL-1β expression (60–62); therefore, the singular overexpression of IL-1α in both PVA and PVP 24-h lavage samples may not be a sufficient indicator of inflammatory response. Additionally, PEO 72-h tissue samples demonstrated increased expression of both MCP-1 and MIP-1, which causes increased localization of neutrophils (63–65); however, no increased neutrophil accumulation was observed in histology samples during this period.

In comparison to experimental groups, the sham-treated control group, in which sterile tweezers were used to mimic the method of fiber administration, showed cytokine profiles similar to those of blank fiber-treated tissue, with a slight increase in neutrophil accumulation in some histological sample replicates. These results suggest that this method of delivery may cause damage to the murine reproductive tract. While previous studies used positive displacement pipettes to intravaginally administer rolled fibers, the amount of fiber administered with this method is limited (25). We believe that the method of administration may be partially responsible for the observed increased cytokine expression, as well as the increased neutrophil accumulation seen in one of the blank PVA histology replicates (Fig. S2A). Future studies will be conducted using alternative methods of fiber administration to assess the impact of administration methods and to more closely represent more commonly used tampon-like administration packages. Moreover, a more in-depth safety study may be conducted in future work to evaluate the dose-dependent safety profile of rapid-release fibers in combination with GRFT.

Concurrent with testing rapid-release GRFT fibers, N-9 gel was used as a positive control in our *in vivo* safety studies (21). However, histology samples showed that a single administration of N-9 only marginally increased neutrophil accumulation in tissue, and no marked increase was observed in cytokine expression relative to that in untreated or blank fiber-treated mice (Fig. 7 and Fig. S2B and S3). Previous studies using N-9 gels have shown that a single administration may result in transient damage within murine reproductive tissue, with the highest severity 4 h postadministration, followed by nearly complete recovery after 24 h (66). This correlates with our *in vivo* safety results, in that mice given a single application of N-9 gel showed minimal damage at the time points assessed (24 and 72 h). Future studies will assess long-term safety using multiple administrations of GRFT fibers and N-9 gel.

While we acknowledge the lack of a GRFT fiber group in these initial toxicity studies, we predict that GRFT fibers will exhibit safety profiles similar to that observed with free GRFT based on several factors. First, our *in vitro* safety assays that tested 10% (wt/wt) GRFT fibers (at 2.5 mg/ml) showed no decrease in viability across 5 different cell lines following GRFT fiber administration. Moreover, previous studies have already demonstrated the longer-term safety of free GRFT within a range of concentrations (0.05 to 0.25 mg of GRFT and 1 to 4 μM GRFT) both *in vitro* and *in vivo* with multiple administrations for up to 2 weeks (22, 67). We would expect that *in vivo* GRFT fibers with similar dosages (here 5-mg fibers equating to 0.5 mg of GRFT) will provide results similar to those of our *in vitro* and previously described *in vivo* safety assays.

From a polymer perspective, previous studies have shown that the administration of polymers or agents that induce an inflammatory response within the FRT typically result in increased viral infection (68). In contrast, our studies demonstrated that blank rapid-release fibers decreased HSV-2 infection in mice compared to that in untreated infected mice, indicating that polymer alone will not contribute to infectivity. Moreover, for the GRFT fiber groups, mice demonstrated prolonged survival relative to those with both blank fibers and untreated infected controls as well, providing some indication of decreased susceptibility and less inflammation. The safety results from our blank fibers are in line with the established biocompatibility and FDA approval of these polymers for active-agent delivery (69–71).

In these studies, we have fabricated rapid-release GRFT fibers to provide on-demand

protection against HIV-1 and HSV-2 infections and have demonstrated the preliminary safety of GRFT fibers. Our goal is to create a delivery platform providing women an alternative viable solid dosage form that offers dual protection against STIs. Based on our cytokine work, future preclinical studies will explore alternative administration methods to ensure that platform administration does not enhance susceptibility to viral infection or cause off-target effects. Furthermore, the interaction between rapid-release fibers and the vaginal mucosa may be investigated to fully rule out the potential of these platforms to elicit cytotoxic effects, while additional studies will examine the window of protection and dose-dependent response imparted by challenging with HSV-2 at different time points with respect to fiber administration. Moreover, we anticipate that GRFT fibers may enhance retention within the reproductive tract, and in future work, we plan to study the retention and pharmacokinetics of GRFT delivered from these fibers after different durations and how these concentration profiles relate to protection. Last, we anticipate that these rapid-release fibers may be used as a foundation to develop sustained-release multilayered fibers, which may provide extended release, decreased doses, and potentially increased user adherence relative to existing delivery platforms.

MATERIALS AND METHODS

Materials. PEO (molecular weight [MW], 600,000), PVA (87 to 90% hydrolyzed; MW, 30,000 to 70,000), and PVP (MW, 1,400,000) were purchased from Sigma-Aldrich (St. Louis, MO). Organic solvents, including dimethyl sulfoxide (DMSO), were also purchased from Sigma-Aldrich. Cell culture media and reagents, including Dulbecco's modified Eagle medium (DMEM), minimum essential medium (MEM), fetal bovine serum (FBS), penicillin, streptomycin, and HEPES, were purchased from VWR (Radnor, PA). Keratinocyte serum-free medium (KSFM) and gentamicin were purchased from Thermo Fisher (Hampton, NH). Griffithsin stock solution (12.0 mg/ml in phosphate-buffered saline [PBS]) was manufactured in *Nicotiana benthamiana* following methods previously described by our group (15, 72).

Cell lines and virus. TZM-bl cells, obtained from the National Institutes of Health (NIH) AIDS Reagent Program, were used to assess *in vitro* HIV-1 infectivity. TZM-bl cells are engineered HeLa cells that express CD4, CCR5, and CXCR4 receptors and contain a Tat-driven luciferase gene, which is activated by HIV-1 infection and permits sensitive and accurate measurements of infection. TZM-bl cells are highly permissive to infection by most strains of HIV and molecularly cloned Env-pseudotyped viruses. TZM-bl cells were cultured in DMEM containing 10% FBS, 25 mM HEPES, and 50 μg/ml of gentamicin.

The Env-pseudotyped HIV-1 was produced in-house by transducing HEK-293T/17 cells with both an envelope (Env)-expressing plasmid (CCR5-tropic clade A strain Q769.h5) and an Env-deficient HIV-1 backbone vector (pNL4.3ΔEnv-Luc). Both plasmids were obtained from the NIH AIDS Reagent Program (catalog numbers 11884 and 3418). HEK-293T (human embryonic kidney) cells were purchased from the ATCC (Manassas, VA). Cells were maintained in MEM supplemented with 10% FBS, penicillin (100 μg/ml), and streptomycin (100 μg/ml).

HSV-2 infection was assessed in plaque assays in Vero E6 cells (African green monkey kidney cells). HSV-2 (4674) was kindly provided by Betsy Herold from Albert Einstein College of Medicine. Cells were maintained in MEM supplemented with 10% FBS, penicillin (100 μg/ml), and streptomycin (100 μg/ml).

Finally, vaginal keratinocyte (VK2/E6E7), ectocervical (Ect1/E6E7), and endocervical (End1/E6E7) cell lines, as well as TZM-bl and Vero E6 cell lines, were used to assess fiber cytotoxicity (all vaginal cells were originally from the ATCC). VK2/E6E7 (VK2), Ect1/E6E7 (Ect1), and End1/E6E7 (End1) are well-characterized immortalized cell lines derived from normal human vaginal, ectocervical, and endocervical epithelia, respectively, which are representative of the cell types found within the FRT. Cells were maintained in KSFM supplemented with recombinant human epidermal growth factor (0.1 ng/ml), bovine pituitary extract (50 μg/ml), calcium chloride (0.4 mM), and 1% penicillin and streptomycin (100 μg/ml each). During cell trypsinization, plating, and counting, cells were neutralized with 1:1 DMEM-KSFM (with 10% FBS and 1% penicillin/streptomycin [100 μg/ml each]).

Rapid-release-fiber fabrication. Hydrophilic polymer solutions were fabricated by first weighing polymer into a glass scintillation vial and incubating it overnight in 1 ml of Milli-Q water. To create PVA and PVP fibers with well-defined morphologies, 200 mg of either PVA or PVP were added to 1 ml of Milli-Q water (20% [wt/vol] solution), while PEO fibers were fabricated by adding 50 mg of polymer to 1 ml of Milli-Q water (5% [wt/vol]). Blank fibers were electrospun with a mandrel-to-syringe distance of 20 cm, flow rate of 0.2 to 0.3 ml, and a voltage of 15 kV. The flow rate and voltage were changed to 0.2 ml/h and 25 kV for 1 and 10% (wt/wt) (GRFT-to-polymer weight ratio) GRFT fibers.

Fiber morphology. The morphology of blank PEO, PVA, and PVP fibers, as well as 1% and 10% GRFT (wt/wt) PEO, PVA, and PVP fibers, was assessed using scanning electron microscopy (SEM). After electrospinning, fibers were dried for 24 h in a desiccator, cut into 5-mm pieces, and placed on double-sided adhesive carbon tabs (Ted Pella Inc., Redding, CA), which were adhered to aluminum stubs. The adhered fiber pieces were sputter coated with a thin gold alloy film using a Bio-Rad (Hercules, CA) E5100 sputter coat system. The coating process was operated for 90 s at 20 mA. Multiple SEM images were acquired using a Supra 35 SEM (Zeiss, Oberkochen, Germany), with images captured under an accelerating voltage of 8 kV and using an average magnification of ×1,000 to ×5,000. The average fiber

diameter was determined with ImageJ software (NIH, Bethesda, MD), and a minimum of 50 fibers were assessed per image.

Fiber characterization. To assess GRFT loading, PEO, PVA, and PVP fibers were weighed (3 to 5 mg) into separate 1.5-ml Eppendorf tubes, followed by the addition of 1 ml of PBS. After 1 to 2 min, the dissolved fiber solutions were vortexed and analyzed using ELISA to quantify GRFT loading and encapsulation efficiency (defined as [actual loading/theoretical loading] $\times$ 100).

The ELISA was conducted using 96-well Nunc Maxisorp plates as previously described (37). Briefly, plates were first prepared by coating wells with 100 μl of gp120 (250 ng/ml) in PBS and incubating them overnight at 4°C. Afterward, the coating buffer was removed and 300 μl of blocking buffer, consisting of PBS with 0.05% (vol/vol) Tween 20 (PBST) and 3% (wt/vol) bovine serum albumin, was added to each well. Plates were incubated at room temperature for 2 h and then washed three times with PBST using a Multiwash III plate washer (Gardner Denver, Milwaukee, WI). One-hundred-microliter volumes of GRFT standards (ranging from 0.2 to 120 ng/ml) and loading extracts were added to each well and incubated for 1 h h at 37°C. Dilutions of goat anti-GRFT primary antibody (1:10,000, provided by Kenneth Palmer, University of Louisville) and rabbit anti-goat IgG-horseradish peroxidase (HRP) secondary antibody (1:20,000; Sigma-Aldrich) were added in volumes of 100 μl and each incubated for 1 h at 37°C to detect bound GRFT. Finally, 100 μl of KPL SureBlue tetramethylbenzidine (TMB) microwell peroxidase substrate (Sera Care, Milford, MA) was added to each well for 90 s, and the reaction was quenched with the addition of 100 μl of 1 N H_2SO_4 (Thermo Fisher, Waltham, MA). Plate absorbance was measured at 450 nm on a Synergy HT reader (BioTek, Winooski, VT). Data were analyzed using Prism (version 6.0; GraphPad Software, La Jolla, CA).

***In vitro* HIV-1 pseudovirus inhibition assay.** The antiviral activity of GRFT fibers against HIV-1 was measured using an *in vitro* HIV-1 pseudovirus inhibition assay. As previously described (33, 37, 38), HIV-1 inhibition was determined as a function of reduction in luciferase reporter gene expression after a single round of infection in TZM-bl cells. The optimal virus dilution was established prior to the experiments to yield ~100,000 relative luminescence units (RLUs).

Briefly, 1% GRFT fibers (~3 to 5 mg) were first dissolved in sterile PBS, followed by serial dilutions (1:2) with DMEM to a final volume of 50 μl within a 96-well plate. Rapid-release-fiber eluates and eluate dilutions were used in both HIV-1 and HSV-2 *in vitro* antiviral assays due to their rapid dissolution time (~1 min) and to provide more accurate dosing for viral inhibition experiments than that obtained by using a series of smaller fiber samples. TZM-bl cells (10,000 cells in 100 μl of DMEM with 10 μg/ml of DEAE-dextran) were subsequently added to each well, followed by the addition of 50 μl of diluted HIV-1 pseudovirus. Cells were then incubated at 37°C for 48 h. Dilutions of free GRFT (stock concentration, 50 μg/ml) ranging from 15 pg/ml to 120 ng/ml were similarly prepared for comparison.

After 48 h, 100 μl of culture medium was carefully removed from each well. Luminescence was measured using the Bright-Glo luciferase assay system (Promega Corporation, Madison, WI) by adding 100 μl of Bright-Glo reagent solution to each well for 5 min. Plates were read via luminescence by the Synergy HT reader (BioTek). All RLU values were corrected by subtracting the RLU of untreated uninfected cells from the sample RLUs (treated infected cells). The percent virus inhibition was determined by normalizing the corrected RLUs of treated infected cells to those of corrected untreated infected cells: percent infection = [(sample RLU – untreated uninfected cells)/(untreated infected cells – untreated uninfected cells)] $\times$ 100. The antiviral activity of GRFT fibers is reported as the half-maximal inhibitory concentration (IC_{50}), which was calculated by comparing the untreated infected corrected control RLUs to the corrected RLUs of sample dilutions.

***In vitro* HSV-2 plaque assay.** HSV-2 plaque assays were conducted to evaluate the *in vitro* efficacy of 10% (wt/wt) GRFT fibers against HSV-2 infection as previously described (33). Briefly, Vero E6 cells were seeded at 600,000/well in a 6-well flat-bottom plate (50% confluence) and grown for 24 h to confluence. Prior to cell infection, 10% (wt/wt) GRFT fibers (30 mg) were dissolved in 20 ml of complete plating medium (1% FBS–MEM). Once the cells were fully confluent, the growth medium was removed and replaced with 2 ml of GRFT fiber eluate dilutions, followed by HSV-2 infection (3,000 PFU per well) 1 h later. Free GRFT (2,000 μg/ml), corresponding to the concentration necessary to provide complete HSV-2 inhibition, was used as a positive control for inhibition, in addition to untreated uninfected cells. Untreated infected cells were used as a negative control of inhibition.

Subsequent to HSV-2 infection, plates were incubated for 48 h at 37°C, all medium was removed, and cells were fixed with 1.5 ml of methanol for 10 min. Afterward, 0.1% crystal violet was applied for 30 min to stain the plaques. Finally, plates were washed with Milli-Q water, and plaques were counted after drying. Plaque numbers from experimental groups were normalized relative to the number of plaques in untreated infected cells (~280 to 300 plaques per well). Samples were analyzed in triplicate, and GraphPad Prism software was used to determine the IC_{50} values and compare the IC_{50} values of GRFT fibers to that of free GRFT.

***In vitro* cytotoxicity.** Vaginal epithelial (VK2/E6E7), ectocervical (Ect1/E6E7), and endocervical (End1/E6E7) cells, as well as TZM-bl and Vero E6 cells, were administered either blank or GRFT fibers to assess *in vitro* safety. Cells were plated at a density of 50,000/well in 96-well plates and incubated in triplicate with 0.5-mg fiber pieces placed in the solution (2.5-mg/ml final concentration). While fiber pieces were administered to assess the potential toxicity of the solid dosage form, fibers rapidly dissolved into the surrounding medium within ~1 min. No treatment (medium alone) and 10% DMSO were used as positive and negative controls of cell viability, respectively. After 24, 48, and 72 h, 20 μl of MTT reagent was added to the cells and incubated for an additional 4 h, followed by overnight lysis with the addition of 100 μl of lysis buffer (10% sodium dodecyl sulfate in 0.01 M hydrochloric acid). Absorbance

TABLE 2 GRFT doses administered in fibers or gel during *in vivo* HSV-2 infectivity studies

Formulation name	Amt of vehicle administered per mouse	Total GRFT administered based on loading (μg)
GRFT PEO	5 mg of fiber	420
GRFT PVA	5 mg of fiber	350
GRFT PVP	5 mg of fiber	312
0.1% (wt/vol) GRFT solution	20 μl in PBS	20

measurements (570 nm) were taken the following day. All sample absorbance values were normalized to untreated cell absorbance to obtain percent viability.

In vivo efficacy against a lethal dose of HSV-2 infection. All *in vivo* experimental procedures were approved by the University of Louisville's Institutional Animal Care and Use Committee (IACUC 17135) prior to testing. All animal studies were conducted using 5-week-old female BALB/c mice (Jackson Laboratory, Bar Harbor, ME) to evaluate the efficacy and safety of GRFT fibers. For efficacy studies, mice were administered either blank or GRFT fibers (5 mg) that were UV sterilized for 15 s (Table 2). Mice were subcutaneously injected with 3 mg of Depo-Provera (Revive, Madison, NJ) to induce the diestrous stage of their cycle, 5 days prior to fiber administration.

To determine the efficacy of GRFT fibers against HSV-2 infection, mice were administered a single dose of either GRFT PEO, PVA, or PVP fibers or a control. For efficacy experiments, a total of 20 mice were used per treatment group, across 4 independent studies, each with 5 mice. Four hours after fiber administration, mice were challenged with HSV-2 (20 μl; LD$_{90}$, 5,000 PFU). Untreated infected mice were used as positive controls for infection, while untreated uninfected mice and infected mice treated with free GRFT (20 μl of 1,000 μg/ml, equivalent to 20 μg GRFT) served as negative controls. Free GRFT doses were based on previous studies with GRFT gels that were shown to provide *in vivo* protection against HSV-2 infection (21). Blank PEO fibers were administered as an additional control group in efficacy studies. Mice were monitored daily for 14 days after HSV-2 challenge using an established 4-point scale to monitor the progression of viral infection (22, 73). Each day, mice were weighed and examined for signs of neurological and epithelial damage. After the 2-week period following HSV-2 challenge, mice were euthanized and Kaplan-Meier survival curves were generated. Log-ranked *post hoc* tests were conducted to assess the statistical significance between groups.

In vivo safety. To assess the safety of fiber administration, two separate studies were conducted to assess tissue histology and cytokine expression in murine reproductive tracts following fiber administration. Similar to the case with efficacy experiments, mice were subcutaneously injected with 3 mg of Depo-Provera 5 days prior to fiber administration. Both histology and cytokine studies used 3 mice per treatment group per time point to evaluate the preliminary safety of fiber administration. Afterward, UV-sterilized blank fibers (5 mg) were intravaginally administered to mice under isoflurane anesthesia using sterile tweezers. Treatment groups included mice administered blank PEO, PVA, or PVP fibers, while control groups included untreated mice or mice treated with 20 μl of free GRFT in PBS (1,000 μg/ml) or 40 μl of Conceptrol gel. An additional sham control was used to mimic fiber administration using tweezers alone. Mice ($n = 3$ per time point) were euthanized 24 or 72 h after fiber administration, and mouse reproductive tracts and vaginal lavage samples were collected and stored at $-80°C$ following euthanasia.

In the first study, the structural integrity of collected reproductive tracts was evaluated using histological analysis. First, tissue samples were washed with PBS, followed by fixation with 4% paraformaldehyde. Samples were then embedded in a paraffin block and stained with hematoxylin and eosin (H&E; staining was performed by the Pathology Core Research Laboratory at the University of Louisville). Sample cross sections ($n = 3$ per group per time point) were analyzed by a pathologist blinded to the treatment groups.

A separate study was conducted to determine cytokine levels after blank fiber administration. All murine reproductive tracts and vaginal lavage samples were assessed using a Luminex assay. First, 20 μl of T-Per solution (Thermo Fisher) containing 1% Halt protease inhibitor cocktail (Thermo Fisher) was added per milligram of reproductive tissue. Approximately 20 zirconia/silica beads (BioSpec Productions) were added to each sample, followed by homogenization at 4,500 rpm for 180 s using Precellys 24 homogenizer (Bertin, France). Homogenized samples were cooled on ice for 5 min and centrifuged at 10,000 × g at 4°C for 5 min. Afterward, sample supernatants were collected, aliquoted, and stored at $-80°C$ for further study. Prior to conducting the Luminex assay, interleukin-1β (IL-1β) levels were tested in reproductive tissue samples using specific ELISA Ready-SET-Go! kits (Thermo Fisher). Finally, Luminex assays were used to quantify the cytokine levels in collected mouse tissue and lavage samples. Cytokines, including granulocyte colony-stimulating factor (G-CSF), IFN-γ, IL-1α, IL-1β, IL-2, IL-6, IP-10, MCP-1, MIP-1α, MIP1-β, MIP-2, and tumor necrosis factor alpha (TNF-α), were selected based on previous studies that examined these markers for intravaginal inflammation and damage (21, 22).

Statistical analysis. Unless otherwise noted, all *in vitro* experiments were conducted in triplicate, with a minimum of 3 replicates per sample ($n = 3$). Statistical analysis of samples assessing fiber morphology, fiber characterization, *in vitro* assays, and *in vivo* safety studies was performed by using one-way analysis of variance (ANOVA) with the Bonferroni *post hoc* test ($P < 0.05$). For murine studies assessing viral efficacy, log-ranked *post hoc* tests were conducted to assess statistical significance as a function of treatment group and survival outcome.

SUPPLEMENTAL MATERIAL

Supplemental material is available online only.

SUPPLEMENTAL FILE 1, PDF file, 0.4 MB.

ACKNOWLEDGMENTS

REFERENCES

1. UNAIDS. 2015. How AIDS changed everything—MDG6: 15 years, 15 lessons of hope from the AIDS response. UNAIDS, Geneva, Switzerland.
2. UNAIDS. 2018. Fact sheet—latest statistics on the status of the AIDS epidemic. http://www.unaids.org/en/resources/fact-sheet.
3. Freeman EE, Weiss HA, Glynn JR, Cross PL, Whitworth JA, Hayes RJ. 2006. Herpes simplex virus 2 infection increases HIV acquisition in men and women: systematic review and meta-analysis of longitudinal studies. AIDS 20:73–83. https://doi.org/10.1097/01.aids.0000198081.09337.a7.
4. Corey L, Wald A, Celum CL, Quinn TC. 2004. The effects of herpes simplex virus-2 on HIV-1 acquisition and transmission: a review of two overlapping epidemics. J Acquir Immune Defic Syndr 35:435–445. https://doi.org/10.1097/00126334-200404150-00001.
5. Holt M, Murphy DA, Callander D, Ellard J, Rosengarten M, Kippax SC, de Wit J. 2012. Willingness to use HIV pre-exposure prophylaxis and the likelihood of decreased condom use are both associated with unprotected anal intercourse and the perceived likelihood of becoming HIV positive among Australian gay and bisexual men. Sex Transm Infect 88:258–263. https://doi.org/10.1136/sextrans-2011-050312.
6. Hurt CB, Eron JJ, Cohen MS. 2011. Pre-exposure prophylaxis and antiretroviral resistance: HIV prevention at a cost? Clin Infect Dis 53:1265–1270. https://doi.org/10.1093/cid/cir684.
7. Krogstad EA, Rathbone MJ, Woodrow KA. 2014. Vaginal drug delivery, p 607–651. In Domb AJ, Khan W (ed), Focal controlled drug delivery. Springer US, Boston, MA.
8. Montgomery ET, Mensch B, Musara P, Hartmann M, Woeber K, Etima J, van der Straten A. 2017. Misreporting of product adherence in the MTN-003/VOICE trial for HIV prevention in Africa: participants' explanations for dishonesty. AIDS Behav 21:481–491. https://doi.org/10.1007/s10461-016-1609-1.
9. Van Damme L, Corneli A, Ahmed K, Agot K, Lombaard J, Kapiga S, Malahleha M, Owino F, Manongi R, Onyango J, Temu L, Monedi MC, Mak'Oketch P, Makanda M, Reblin I, Makatu SE, Saylor L, Kiernan H, Kirkendale S, Wong C, Grant R, Kashuba A, Nanda K, Mandala J, Fransen K, Deese J, Crucitti T, Mastro TD, Taylor D, Grp F-P. 2012. Preexposure prophylaxis for HIV infection among African women. N Engl J Med 367:411–422. https://doi.org/10.1056/NEJMoa1202614.
10. McMahon JM, Myers JE, Kurth AE, Cohen SE, Mannheimer SB, Simmons J, Pouget ER, Trabold N, Haberer JE. 2014. Oral pre-exposure prophylaxis (PrEP) for prevention of HIV in serodiscordant heterosexual couples in the United States: opportunities and challenges. AIDS Patient Care STDS 28:462–474. https://doi.org/10.1089/apc.2013.0302.
11. Tetteh RA, Yankey BA, Nartey ET, Lartey M, Leufkens HG, Dodoo AN. 2017. Pre-exposure prophylaxis for HIV prevention: safety concerns. Drug Saf 40:273–283. https://doi.org/10.1007/s40264-017-0505-6.
12. Alexandre KB, Gray ES, Mufhandu H, McMahon JB, Chakauya E, O'Keefe BR, Chikwamba R, Morris L. 2012. The lectins griffithsin, cyanovirin-N and scytovirin inhibit HIV-1 binding to the DC-SIGN receptor and transfer to CD4(+) cells. Virology 423:175–186. https://doi.org/10.1016/j.virol.2011.12.001.
13. Huskens D, Vermeire K, Vandemeulebroucke E, Balzarini J, Schols D. 2008. Safety concerns for the potential use of cyanovirin-N as a microbicidal anti-HIV agent. Int J Biochem Cell Biol 40:2802–2814. https://doi.org/10.1016/j.biocel.2008.05.023.
14. Mori T, O'Keefe BR, Sowder RC, Bringans S, Gardella R, Berg S, Cochran P, Turpin JA, Buckheit RW, McMahon JB, Boyd MR. 2005. Isolation and characterization of griffithsin, a novel HIV-inactivating protein, from the red alga Griffithsia sp. J Biol Chem 280:9345–9353. https://doi.org/10.1074/jbc.M411122200.
15. O'Keefe BR, Vojdani F, Buffa V, Shattock RJ, Montefiori DC, Bakke J, Mirsalis J, d'Andrea A-L, Hume SD, Bratcher B, Saucedo CJ, McMahon JB, Pogue GP, Palmer KE. 2009. Scaleable manufacture of HIV-1 entry inhibitor griffithsin and validation of its safety and efficacy as a topical microbicide component. Proc Natl Acad Sci U S A 106:6099–6104. https://doi.org/10.1073/pnas.0901506106.
16. Meuleman P, Albecka A, Belouzard S, Vercauteren K, Verhoye L, Wychowski C, Leroux-Roels G, Palmer KE, Dubuisson J. 2011. Griffithsin has antiviral activity against hepatitis C virus. Antimicrob Agents Chemother 55:5159–5167. https://doi.org/10.1128/AAC.00633-11.
17. Levendosky K, Mizenina O, Martinelli E, Jean-Pierre N, Kizima L, Rodriguez A, Kleinbeck K, Bonnaire T, Robbiani M, Zydowsky TM, O'Keefe BR, Fernández-Romero JA. 2015. Griffithsin and carrageenan combination to target herpes simplex virus 2 and human papillomavirus. Antimicrob Agents Chemother 59:7290–7298. https://doi.org/10.1128/AAC.01816-15.
18. O'Keefe BR, Giomarelli B, Barnard DL, Shenoy SR, Chan PKS, McMahon JB, Palmer KE, Barnett BW, Meyerholz DK, Wohlford-Lenane CL, McCray PB. 2010. Broad-spectrum in vitro activity and in vivo efficacy of the antiviral protein griffithsin against emerging viruses of the family Coronaviridae. J Virol 84:2511–2521. https://doi.org/10.1128/JVI.02322-09.
19. Barton C, Kouokam JC, Lasnik AB, Foreman O, Cambon A, Brock G, Montefiori DC, Vojdani F, McCormick AA, O'Keefe BR, Palmer KE. 2014. Activity of and effect of subcutaneous treatment with the broad-spectrum antiviral lectin griffithsin in two laboratory rodent models. Antimicrob Agents Chemother 58:120–127. https://doi.org/10.1128/AAC.01407-13.
20. Emau P, Tian B, O'Keefe BR, Mori T, McMahon JB, Palmer KE, Jiang Y, Bekele G, Tsai CC. 2007. Griffithsin, a potent HIV entry inhibitor, is an excellent candidate for anti-HIV microbicide. J Med Primatol 36:244–253. https://doi.org/10.1111/j.1600-0684.2007.00242.x.
21. Nixon B, Stefanidou M, Mesquita PMM, Fakioglu E, Segarra T, Rohan L, Halford W, Palmer KE, Herold BC. 2013. Griffithsin protects mice from genital herpes by preventing cell-to-cell spread. J Virol 87:6257–6269. https://doi.org/10.1128/JVI.00012-13.
22. Kouokam JC, Huskens D, Schols D, Johannemann A, Riedell SK, Walter W, Walker JM, Matoba N, O'Keefe BR, Palmer KE. 2011. Investigation of griffithsin's interactions with human cells confirms its outstanding safety and efficacy profile as a microbicide candidate. PLoS One 6:e22635. https://doi.org/10.1371/journal.pone.0022635.
23. Skoler-Karpoff S, Ramjee G, Ahmed K, Altini L, Plagianos MG, Friedland B, Govender S, De Kock A, Cassim N, Palanee T, Dozier G, Maguire R, Lahteenmaki P. 2008. Efficacy of Carraguard for prevention of HIV infection in women in South Africa: a randomised, double-blind, placebo-controlled trial. Lancet 372:1977–1987. https://doi.org/10.1016/S0140-6736(08)61842-5.
24. Marrazzo JM, Ramjee G, Richardson BA, Gomez K, Mgodi N, Nair G, Palanee T, Nakabiito C, van der Straten A, Noguchi L, Hendrix CW, Dai JY, Ganesh S, Mkhize B, Taljaard M, Parikh UM, Piper J, Mâsse B, Grossman C, Rooney J, Schwartz JL, Watts H, Marzinke MA, Hillier SL, McGowan IM, Chirenje ZM. 2015. Tenofovir-based preexposure prophylaxis for HIV infection among African women. N Engl J Med 372:509–518. https://doi.org/10.1056/NEJMoa1402269.
25. Krogstad EA, Ramanathan R, Nhan C, Kraft JC, Blakney AK, Cao S, Ho RJY, Woodrow KA. 2017. Nanoparticle-releasing nanofiber composites for

enhanced in vivo vaginal retention. Biomaterials 144:1–16. https://doi .org/10.1016/j.biomaterials.2017.07.034.

26. Huang CB, Soenen SJ, van Gulck E, Vanham G, Rejman J, Van Calenbergh S, Vervaet C, Coenye T, Verstraelen H, Temmerman M, Demeester J, De Smedt SC. 2012. Electrospun cellulose acetate phthalate fibers for semen induced anti-HIV vaginal drug delivery. Biomaterials 33:962–969. https:// doi.org/10.1016/j.biomaterials.2011.10.004.

27. Ball C, Krogstad E, Chaowanachan T, Woodrow KA. 2012. Drug-eluting fibers for HIV-1 inhibition and contraception. PLoS One 7:e49792. https://doi.org/10.1371/journal.pone.0049792.

28. Carson D, Jiang Y, Woodrow KA. 2016. Tunable release of multiclass anti-HIV drugs that are water-soluble and loaded at high drug content in polyester blended electrospun fibers. Pharm Res 33:125–136. https:// doi.org/10.1007/s11095-015-1769-0.

29. Ball C, Woodrow KA. 2014. Electrospun solid dispersions of maraviroc for rapid intravaginal preexposure prophylaxis of HIV. Antimicrob Agents Chemother 58:4855–4865. https://doi.org/10.1128/AAC.02564-14.

30. Blakney AK, Krogstad EA, Jiang YH, Woodrow KA. 2014. Delivery of multipurpose prevention drug combinations from electrospun nanofi- bers using composite microarchitectures. Int J Nanomedicine 9:2967–2978. https://doi.org/10.2147/IJN.S61664.

31. Ball C, Chou SF, Jiang Y, Woodrow KA. 2016. Coaxially electrospun fiber-based microbicides facilitate broadly tunable release of maraviroc. Mater Sci Eng C Mater Biol Appl 63:117–124. https://doi.org/10.1016/j .msec.2016.02.018.

32. Blakney AK, Ball C, Krogstad EA, Woodrow KA. 2013. Electrospun fibers for vaginal anti-HIV drug delivery. Antiviral Res 100:S9–S16. https://doi .org/10.1016/j.antiviral.2013.09.022.

33. Tyo KM, Vuong HR, Malik DA, Sims LB, Alatassi H, Duan JH, Watson WH, Steinbach-Rankins JM. 2017. Multipurpose tenofovir disoproxil fumarate electrospun fibers for the prevention of HIV-1 and HSV-2 infections in vitro. Int J Pharm 531:118–133. https://doi.org/10.1016/j.ijpharm.2017 .08.061.

34. Aniagyei SE, Sims LB, Malik DA, Tyo KM, Curry KC, Kim W, Hodge DA, Duan J, Steinbach-Rankins JM. 2017. Evaluation of poly(lactic-co-glycolic acid) and poly(dl-lactide-co-epsilon-caprolactone) electrospun fibers for the treatment of HSV-2 infection. Mater Sci Eng C Mater Biol Appl 72:238–251. https://doi.org/10.1016/j.msec.2016.11.029.

35. Derby N, Lal M, Aravantinou M, Kizima L, Barnable P, Rodriguez A, Lai M, Wesenberg A, Ugaonkar S, Levendosky K, Mizenina O, Kleinbeck K, Lifson JD, Peet MM, Lloyd Z, Benson M, Heneine W, O'Keefe BR, Robbiani M, Martinelli E, Grasperge B, Blanchard J, Gettie A, Teleshova N, Fernández- Romero JA, Zydowsky TM. 2018. Griffithsin carrageenan fast dissolving inserts prevent SHIV HSV-2 and HPV infections in vivo. Nat Commun 9:3881. https://doi.org/10.1038/s41467-018-06349-0.

36. Lal M, Lai M, Ugaonkar S, Wesenberg A, Kizima L, Rodriguez A, Leven- dosky K, Mizenina O, Fernández-Romero J, Zydowsky T. 2018. Develop- ment of a vaginal fast-dissolving insert combining griffithsin and carra- geenan for potential use against sexually transmitted infections. J Pharm Sci 107:2601–2610. https://doi.org/10.1016/j.xphs.2018.06.002.

37. Tyo KM, Duan J, Kollipara P, Dela Cerna MVC, Lee D, Palmer KE, Steinbach-Rankins JM. 2019. pH-responsive delivery of griffithsin from electrospun fibers. Eur J Pharm Biopharm 138:64–74. https://doi.org/10 .1016/j.ejpb.2018.04.013.

38. Grooms TN, Vuong HR, Tyo KM, Malik DA, Sims LB, Whittington CP, Palmer KE, Matoba N, Steinbach-Rankins JM. 2016. Griffithsin-modified electrospun fibers as a delivery scaffold to prevent HIV infection. Anti- microb Agents Chemother 60:6518–6531. https://doi.org/10.1128/AAC .00956-16.

39. Beumer GJ, van Blitterswijk CA, Bakker D, Ponec M. 1993. Cell-seeding and in vitro biocompatibility evaluation of polymeric matrices of PEO/ PBT copolymers and PLLA. Biomaterials 14:598–604. https://doi.org/10 .1016/0142-9612(93)90178-5.

40. Hago E-E, Li X. 2013. Interpenetrating polymer network hydrogels based on gelatin and PVA by biocompatible approaches: synthesis and char- acterization. Adv Mater Sci Eng 2013:1–8. https://doi.org/10.1155/2013/ 328763.

41. Singh B, Pal L. 2012. Sterculia crosslinked PVA and PVA-poly(AAm) hydrogel wound dressings for slow drug delivery: mechanical, mucoad- hesive, biocompatible and permeability properties. J Mech Behav Biomed Mater 9:9–21. https://doi.org/10.1016/j.jmbbm.2012.01.021.

42. Rogero SO, Malmonge SM, Lugão AB, Ikeda TI, Miyamaru L, Cruz ÁS. 2003. Biocompatibility study of polymeric biomaterials. Artif Organs 27:424–427. https://doi.org/10.1046/j.1525-1594.2003.07249.x.

43. Yang H, Li J, Patel SK, Palmer KE, Devlin B, Rohan LC. 2019. Design of poly(lactic-co-glycolic acid) (PLGA) nanoparticles for vaginal co-delivery of griffithsin and dapivirine and their synergistic effect for HIV prophylaxis. Pharmaceutics 11:184. https://doi.org/10.3390/pharmaceutics11040184.

44. Shaikh R, Raj Singh TR, Garland MJ, Woolfson AD, Donnelly RF. 2011. Mucoadhesive drug delivery systems. J Pharm Bioall Sci 3:89–100. https://doi.org/10.4103/0975-7406.76478.

45. Valenta C. 2005. The use of mucoadhesive polymers in vaginal delivery. Adv Drug Deliv Rev 57:1692–1712. https://doi.org/10.1016/j.addr.2005 .07.004.

46. Apicella A, Cappello B, Del Nobile MA, La Rotonda MI, Mensitieri G, Nicolais L. 1993. Poly(ethylene oxide) (PEO) and different molecular weight PEO blends monolithic devices for drug release. Biomaterials 14:83–90. https://doi.org/10.1016/0142-9612(93)90215-N.

47. Li J, Li X, Ni X, Wang X, Li H, Leong KW. 2006. Self-assembled supramo- lecular hydrogels formed by biodegradable PEO–PHB–PEO triblock co- polymers and α-cyclodextrin for controlled drug delivery. Biomaterials 27:4132–4140. https://doi.org/10.1016/j.biomaterials.2006.03.025.

48. Jeong B, Choi YK, Bae YH, Zentner G, Kim SW. 1999. New biodegradable polymers for injectable drug delivery systems. J Control Release 62: 109–114. https://doi.org/10.1016/S0168-3659(99)00061-9.

49. Desai SD, Blanchard J. 1998. In vitro evaluation of pluronic F127-based controlled-release ocular delivery systems for pilocarpine. J Pharm Sci 87:226–230. https://doi.org/10.1021/js970090e.

50. Wang L, Chang M-W, Ahmad Z, Zheng H, Li J-S. 2017. Mass and con- trolled fabrication of aligned PVP fibers for matrix type antibiotic drug delivery systems. Chem Eng J 307:661–669. https://doi.org/10.1016/j.cej .2016.08.135.

51. Pal K, Banthia AK, Majumdar DK. 2007. Preparation and characteriza- tion of polyvinyl alcohol-gelatin hydrogel membranes for biomedical applications. AAPS PharmSciTech 8:E142–E146. https://doi.org/10 .1208/pt080121.

52. Li X, Kanjwal MA, Lin L, Chronakis IS. 2013. Electrospun polyvinyl-alcohol nanofibers as oral fast-dissolving delivery system of caffeine and ribo- flavin. Colloids Surf B Biointerfaces 103:182–188. https://doi.org/10 .1016/j.colsurfb.2012.10.016.

53. Jeong B, Bae YH, Lee DS, Kim SW. 1997. Biodegradable block copolymers as injectable drug-delivery systems. Nature 388:860–862. https://doi .org/10.1038/42218.

54. Wen P, Wen Y, Zong MH, Linhardt RJ, Wu H. 2017. Encapsulation of bioactive compound in electrospun fibers and its potential applica- tion. J Agric Food Chem 65:9161–9179. https://doi.org/10.1021/acs .jafc.7b02956.

55. Seif S, Planz V, Windbergs M. 2017. Delivery of therapeutic proteins using electrospun fibers—recent developments and current challenges. Arch Pharm Chem Life Sci 350:1700077. https://doi.org/10.1002/ardp .201700077.

56. Vermani K, Garg S. 2000. The scope and potential of vaginal drug delivery. Pharm Sci Technol Today 3:359–364. https://doi.org/10.1016/ S1461-5347(00)00296-0.

57. Ji W, Yang F, Seyednejad H, Chen Z, Hennink WE, Anderson JM, van den Beucken JJ, Jansen JA. 2012. Biocompatibility and degradation charac- teristics of PLGA-based electrospun nanofibrous scaffolds with nanoapa- tite incorporation. Biomaterials 33:6604–6614. https://doi.org/10.1016/j .biomaterials.2012.06.018.

58. Machado A, Cunha-Reis C, Araujo F, Nunes R, Seabra V, Ferreira D, das Neves J, Sarmento B. 2016. Development and in vivo safety assessment of tenofovir-loaded nanoparticles-in-film as a novel vaginal microbicide delivery system. Acta Biomater 44:332–340. https://doi.org/10.1016/j .actbio.2016.08.018.

59. Haider A, Haider S, Kang IK. 2018. A comprehensive review summarizing the effect of electrospinning parameters and potential applications of nanofibers in biomedical and biotechnology. Arabian J Chem 11: 1165–1188. https://doi.org/10.1016/j.arabjc.2015.11.015.

60. Oppenheim JJ, Felmann M, Durum SK, Hirano T, Vilcek J, Nicola NA (ed). 2001. Cytokine reference: a compendium of cytokines and other medi- ators of host defense, vol 1. Ligands. Academic Press, London, United Kingdom.

61. Schindler R, Mancilla J, Endres S, Ghorbani R, Clark SC, Dinarello CA. 1990. Correlations and interactions in the production of interleukin-6 (IL-6), IL-1, and tumor necrosis factor (TNF) in human blood mononu- clear cells: IL-6 suppresses IL-1 and TNF. Blood 75:40–47. https://doi.org/ 10.1182/blood.V75.1.40.40.

62. Ensign LM, Tang BC, Wang Y-Y, Tse TA, Hoen T, Cone R, Hanes J. 2012.

Mucus-penetrating nanoparticles for vaginal drug delivery protect against herpes simplex virus. Sci Transl Med 4:138ra79. https://doi.org/10.1126/scitranslmed.3003453.

63. Matsukawa A, Hogaboam CM, Lukacs NW, Lincoln PM, Strieter RM, Kunkel SL. 2000. Endogenous MCP-1 influences systemic cytokine balance in a murine model of acute septic peritonitis. Exp Mol Pathol 68:77–84. https://doi.org/10.1006/exmp.1999.2296.

64. Deshmane SL, Kremlev S, Amini S, Sawaya BE. 2009. Monocyte chemoattractant protein-1 (MCP-1): an overview. J Interferon Cytokine Res 29:313–326. https://doi.org/10.1089/jir.2008.0027.

65. Cook DN. 1996. The role of MIP-1α in inflammation and hematopoiesis. J Leukoc Biol 59:61–66. https://doi.org/10.1002/jlb.59.1.61.

66. Catalone BJ, Kish-Catalone TM, Budgeon LR, Neely EB, Ferguson M, Krebs FC, Howett MK, Labib M, Rando R, Wigdahl B. 2004. Mouse model of cervicovaginal toxicity and inflammation for preclinical evaluation of topical vaginal microbicides. Antimicrob Agents Chemother 48:1837–1847. https://doi.org/10.1128/AAC.48.5.1837-1847.2004.

67. Kouokam JC, Lasnik AB, Palmer KE. 2016. Studies in a murine model confirm the safety of griffithsin and advocate its further development as a microbicide targeting HIV-1 and other enveloped viruses. Viruses 8:311. https://doi.org/10.3390/v8110311.

68. Galen BT, Martin AP, Hazrati E, Garin A, Guzman E, Wilson SS, Porter DD, Lira SA, Keller MJ, Herold BC. 2007. A comprehensive murine model to evaluate topical vaginal microbicides: mucosal inflammation and susceptibility to genital herpes as surrogate markers of safety. J Infect Dis 195:1332–1339. https://doi.org/10.1086/513279.

69. Qi W, Ghoroghchian PP, Li G, Hammer DA, Therien MJ. 2013. Aqueous self-assembly of poly(ethylene oxide)-block-poly(epsilon-caprolactone) (PEO-b-PCL) copolymers: disparate diblock copolymer compositions give rise to nano- and meso-scale bilayered vesicles. Nanoscale 5:10908. https://doi.org/10.1039/c3nr03250g.

70. Wang X, Yucel T, Lu Q, Hu X, Kaplan DL. 2010. Silk nanospheres and microspheres from silk/pva blend films for drug delivery. Biomaterials 31:1025–1035. https://doi.org/10.1016/j.biomaterials.2009.11.002.

71. Thakur RR, Tekko IA, Al-Shammari F, Ali AA, McCarthy H, Donnelly RF. 2016. Rapidly dissolving polymeric microneedles for minimally invasive intraocular drug delivery. Drug Deliv Transl Res 6:800–815. https://doi.org/10.1007/s13346-016-0332-9.

72. Fuqua JL, Hamorsky K, Khalsa G, Matoba N, Palmer KE. 2015. Bulk production of the antiviral lectin griffithsin. Plant Biotechnol J 13:1160–1168. https://doi.org/10.1111/pbi.12433.

73. Hendrickson BA, Guo J, Brown I, Dennis K, Marcellino D, Hetzel J, Herold BC. 2000. Decreased vaginal disease in J-chain-deficient mice following herpes simplex type 2 genital infection. Virology 271:155–162. https://doi.org/10.1006/viro.2000.0303.